

# Outside-Obstacle Representations with All Vertices on the Outer Face

Oksana Firman ✉ 

Institut für Informatik, Universität Würzburg, Germany

Philipp Kindermann ✉ 

Informatikwissenschaften, Universität Trier, Germany

Jonathan Klawitter ✉ 

School of Computer Science, University of Auckland, New Zealand

Boris Klemz ✉ 

Institut für Informatik, Universität Würzburg, Germany

Felix Klesen ✉ 

Institut für Informatik, Universität Würzburg, Germany

Alexander Wolff  

Institut für Informatik, Universität Würzburg, Germany

---

## Abstract

An *obstacle representation* of a graph  $G$  consists of a set of polygonal obstacles and a drawing of  $G$  as a *visibility graph* with respect to the obstacles: vertices are mapped to points and edges to straight-line segments such that each edge avoids all obstacles whereas each non-edge intersects at least one obstacle. Obstacle representations have been investigated quite intensely over the last few years. Here we focus on *outside-obstacle representations* (OORs) that use only one obstacle in the outer face of the drawing. It is known that every outerplanar graph admits such a representation.

We strengthen this result by showing that every (partial) 2-tree has an OOR. We also consider restricted versions of OORs where the vertices of the graph form a convex or even a regular polygon. We characterize when the complement of a tree and when a complete graph minus a simple cycle admits a convex OOR. We construct regular OORs for all (partial) outerpaths, cactus graphs, and grids.

**2012 ACM Subject Classification** Human-centered computing → Graph drawings; Mathematics of computing → Graph theory

**Keywords and phrases** obstacle representation, visibility graph, outside obstacle

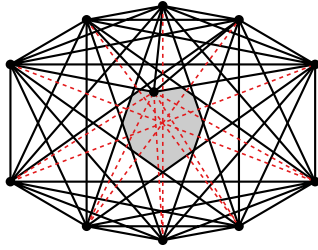
**Related Version** A preliminary version of this work has appeared in Proc. 30th International Symposium Graph Drawing and Network Visualization (GD'22), Springer-Verlag, 2023 [7].

**Funding** *Oksana Firman*: Partially funded by DFG project Wo 758/9-1

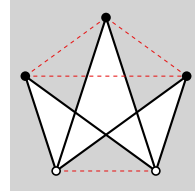
*Jonathan Klawitter*: Beyond Prediction Data Science Research Programme (MBIE grant UOAX1932).

## 1 Introduction

Recognizing graphs that have a certain type of geometric representation is a well-established field of research dealing with, e.g., geometric intersection graphs, visibility graphs, and graphs admitting certain contact representations. Given a set  $\mathcal{C}$  of *obstacles* (here, connected polygonal regions, which we consider to be open) and a set  $P$  of points in the plane, the *visibility graph*  $G_{\mathcal{C}}(P)$  has a vertex for each point in  $P$  and an edge  $pq$  for any two points  $p$  and  $q$  in  $P$  that can *see* each other, that is, the line segment  $\overline{pq}$  connecting  $p$  and  $q$  does not intersect any obstacle in  $\mathcal{C}$  and does not contain any other point of  $P$ . An *obstacle representation* of a graph  $G$  consists of a set  $\mathcal{C}$  of obstacles in the plane and a mapping of the vertices of  $G$  to a set  $P$  of points such that  $G = G_{\mathcal{C}}(P)$ . Note that, in such a representation,



(a) A graph that admits an inside-obstacle representation but no outside-obstacle representation [5].



(b) The complete bipartite graph  $K_{2,3}$  is the smallest graph that contains a cycle and admits an outside-obstacle representation but no inside-obstacle representation [5].

■ **Figure 1** Inside- and outside-obstacle representations of graphs. The gray regions represent the obstacles; the dashed line segments represent the non-edges.

for each *non-edge*  $pq$  of  $G$ , that is, for each non-adjacent vertex pair, the line segment  $\overline{pq}$  *must* intersect an obstacle in  $\mathcal{C}$ . The vertex–point mapping defines a straight-line drawing  $\Gamma$  of  $G_{\mathcal{C}}(P)$ . We planarize  $\Gamma$  by replacing all intersection points by dummy vertices. The faces of this planarization are open polygonal regions. We call the unbounded face the *outer face* of  $\Gamma$ . We differentiate between two types of obstacles: *outside* obstacles lie in the outer face of the drawing, and *inside* obstacles lie in the complement of the outer face; see Figure 1.

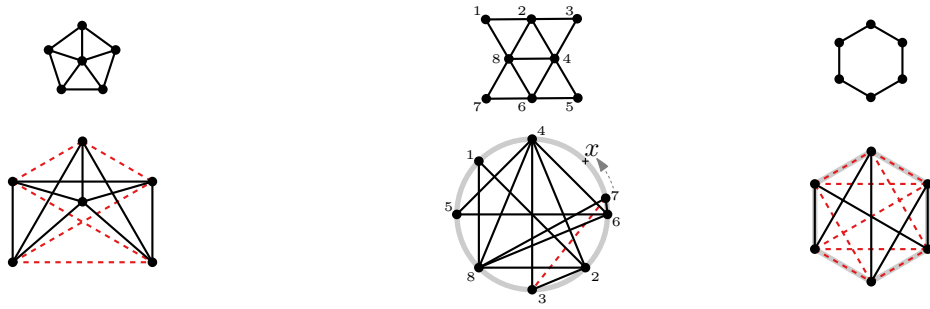
Every graph trivially admits an obstacle representation: take an arbitrary straight-line drawing without collinear vertices and “fill” each face with an obstacle. This, however, can lead to a large number of obstacles, which motivates the optimization problem of finding an obstacle representation with the minimum number of obstacles. For a graph  $G$ , the *obstacle number*  $\text{obs}(G)$  is the smallest number of obstacles that suffice to represent  $G$  as a visibility graph.

While most previous work (discussed below) has focused on establishing bounds for the obstacle number of general graphs, we are interested in understanding which graphs can be represented by a *single* obstacle. In particular, we focus on *outside obstacle representations (OORs)*, that is, obstacle representations with a single outside obstacle and without any inside obstacles. For such a representation, it suffices to specify the positions of the vertices of the given graph; the outside obstacle is simply the whole outer face of the representation. In an OOR, every non-edge of the graph must thus intersect the outer face. We consider three special types of OORs: In a *convex* OOR, the vertices must be in convex position; in a *circular* OOR, the vertices must lie on a circle; and in a *regular* OOR, the vertices must form a regular  $n$ -gon, where  $n$  is the number of vertices of the graph. For examples, refer to Figure 2.

In general, the class of graphs that admit an OOR is not closed under taking subgraphs, but the situation is different for graphs admitting a *reducible* OOR, meaning that all of its edges are incident to the outer face. In this case, we can simply extend the outside obstacle to intersect any edge we want to remove.

► **Observation 1.** *If a graph  $G$  admits a reducible OOR, then every subgraph of  $G$  also admits such a representation.*

**Previous Work.** Alpert, Koch, and Laison [1] introduced the notion of the obstacle number of a graph. They also introduced the notion of an *inside obstacle representations (IOR)*, that is, an obstacle representation without an outside obstacle. They characterized the class of graphs that have an IOR with a single convex obstacle and showed that every outerplanar

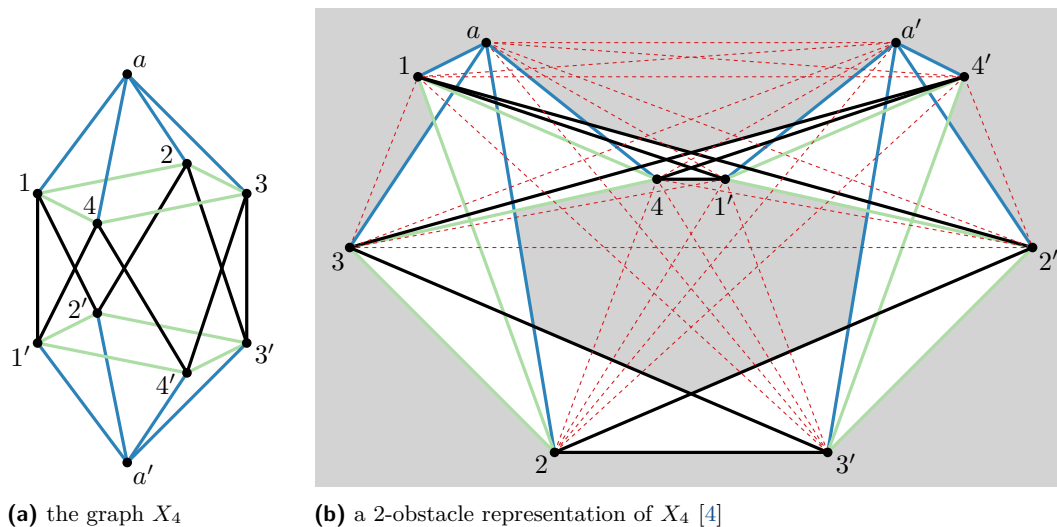


(a) The wheel graph  $W_6$  does not admit a convex OOR (Proposition 11). (b) Graph that admits a circular but not a regular OOR (move vertex 7 towards  $x$ ). (c)  $C_6$  admits a regular OOR.

■ **Figure 2** Non-convex, circular, and regular outside-obstacle representations (OORs). Graph edges are solid black, non-edges are dashed red (in (b) only one non-edge is highlighted).

graph has an OOR. Chaplick, Lipp, Park, and Wolff [5] proved that the class of graphs with an IOR is incomparable with the class of graphs with an OOR by observing that no path admits an IOR and the graph in Figure 1a, which admits an IOR, does not admit an OOR. They showed that any graph with at most seven vertices has an OOR, which does not hold for a specific 8-vertex graph. They also showed that the following *sandwich version* of the outside-obstacle representation problem is NP-hard: Given two graphs  $G$  and  $H$  with the same vertex set  $V$  such that  $G$  is a subgraph of  $H$ , is there a graph  $K$  with vertex set  $V$  that is a supergraph of  $G$  and a subgraph of  $H$  and admits an outside-obstacle representation? Analogous hardness results hold with respect to inside and general obstacles.

Alpert, Koch, and Laison [1] further showed that  $\text{obs}(K_{a,b}^*) \leq 2$  for any  $a \leq b$ , where  $K_{a,b}^*$  is the complete bipartite graph  $K_{a,b}$  minus a matching of size  $a$ . They also proved that  $\text{obs}(K_{5,7}^*) = 2$ . Pach and Sariöz [12] showed that  $\text{obs}(K_{5,5}^*) = 2$ . Berman, Chappell, Faudree, Gimbel, Hartman, and Williams [4] suggested some necessary conditions for a graph to have obstacle number 1. They gave a SAT formula that they used to find a *planar* 10-vertex graph  $X_4$  (of treewidth 4) that has no 1-obstacle representation; see Figure 3.



(a) the graph  $X_4$  (b) a 2-obstacle representation of  $X_4$  [4]

■ **Figure 3** The so-called gyroelongated square bipyramid  $X_4$ , which has treewidth 4, does not admit a representation with a single obstacle.

Obviously, any  $n$ -vertex graph has obstacle number  $\mathcal{O}(n^2)$ . Balko, Cibulka, and Valtr [3] improved this to  $\mathcal{O}(n \log n)$ . On the other hand, Balko, Chaplick, Gupta, Hoffmann, Valtr, and Wolff [2] showed that there are  $n$ -vertex graphs whose obstacle number is  $\Omega(n/\log \log n)$ , improving previous lower bounds, e.g., [1, 6, 10, 11]. They also showed that, when restricting obstacles to *convex* polygons, sometimes a linear number of obstacles is needed. Furthermore, they showed that computing the obstacle number of a graph  $G$  is fixed-parameter tractable in the vertex cover number of  $G$  and that it is NP-hard to decide whether a given graph admits an obstacle representation using a given simple polygon as (outside-) obstacle.

**Contribution.** We do a detailed analysis of the class of graphs that admit OORs: we construct graphs that do not admit convex OORs and we find subclasses that admit convex, circular, or regular OORs. We first strengthen the result of Alpert, Koch, and Laison [1] regarding OORs of outerplanar graphs by showing that every (partial) 2-tree admits a reducible OOR with all vertices on the outer face; see Section 2. Note that, to obtain an OOR of an outerplanar graph  $G$ , we can delete edges from a *reducible* OOR of a 2-tree that contains  $G$  as subgraph. Equivalently, every graph of treewidth at most two, which includes outerplanar and series-parallel graphs, admits such a representation. Note that this result and the above-mentioned 10-vertex planar graph  $X_4$  of treewidth 4 (see Figure 3) that does not admit any 1-obstacle representation [4] leave open the question whether every (planar) graph of treewidth 3 admits an OOR; see our list of open problems in Section 6.

Then we establish two combinatorial conditions for the existence of convex OORs; see Section 3. In particular, we introduce a necessary condition that can be used to show that a given graph does *not* admit a convex OOR as, e.g., the graph  $W_6$  in Figure 2a. We apply these conditions to characterize when the complement of a tree and when a complete graph minus a simple cycle admits a convex OOR. We further construct *regular* reducible OORs for all outerpaths, grids, and cacti; see Section 4. The result for grids strengthens an observation by Dujmović and Morin [6, Fig. 1], who showed that grids have (outside) obstacle number 1.

**Notation.** For a graph  $G$ , let  $V(G)$  be the vertex set of  $G$ , and let  $E(G)$  be the edge set of  $G$ . We use  $n = |V(G)|$  where the graph is clear from the context. Given a cyclic order  $\sigma = \langle v_1, v_2, \dots, v_n \rangle$  of  $V(G)$  and indices  $i$  and  $j$  with  $1 \leq i \neq j \leq n$ , we write  $[v_i, v_j]$  to refer to the subsequence  $\langle v_i, v_{i+1}, \dots, v_{j-1} \rangle$  of  $\sigma$ , where indices are interpreted modulo  $n$ . Subsequences  $(v_i, v_j)$  and  $[v_i, v_j]$  are defined analogously.

## 2 Outside-Obstacle Representations for Partial 2-Trees

The graph class of *2-trees* is recursively defined as follows:  $K_3$  is a 2-tree. Further, any graph is a 2-tree if it is obtained from a 2-tree  $G$  by introducing a new vertex  $x$  and making  $x$  adjacent to both endpoints of some edge  $uv$  in  $G$ . We say that  $x$  is *stacked* on  $uv$  and call the edges  $xu$  and  $xv$  the *parent edges* of  $x$ .

► **Theorem 2.** *Every 2-tree admits a reducible OOR with all vertices on the outer face.*

**Proof.** It follows readily from the definition of 2-trees that every 2-tree  $T$  can be constructed through the following iterative procedure, during which every vertex is marked either as active or inactive. Once a vertex is inactive, it remains inactive for the remainder of the construction.

(S1) Start with some edge, called the *base* edge and mark its vertices as *inactive*. Stack any number of vertices (but at least one vertex) onto the base edge and mark the new vertices as *active*.

(S2) Pick an active vertex  $v$  and stack any number of new vertices (possibly none) onto each of its two parent edges. The new vertices are marked as active and  $v$  is marked as inactive.

(S3) While there are active vertices, repeat step (S2).

Observe that step (S2) is performed exactly once for each vertex that is not incident to the base edge. We construct a drawing of  $T$  by geometrically implementing the iterative procedure described above, so that after every step of the algorithm the present part of the graph is realized as a straight-line drawing satisfying the following set of invariants:

- (I1) Each vertex  $v$  that is not incident to the base edge is associated with an open circular arc  $C_v$  centered at  $v$  that lies completely in the outer face; see Figure 4b. Moreover, the parent edges of  $v$  lie below  $v$  and contain the endpoints of  $C_v$ .
- (I2) Each non-edge intersects the circular arc of at least one of its incident vertices.
- (I3) For each active vertex  $v$ , the region  $R_v$  enclosed by  $C_v$  and the two parent edges of  $v$  (shaded gray in Figure 4b) is *empty*, meaning that  $R_v$  does not contain any vertex of  $T$  and does not intersect any edge or circular arc. (Combined with (I1), it follows that  $R_v$  lies completely in the outer face.)
- (I4) Every vertex is incident to the outer face.

Once the procedure terminates, we have indeed obtained the desired drawing: invariants (I1) and (I2) imply that each non-edge passes through the outer face and, hence, we have indeed obtained an OOR. Moreover, invariant (I1) implies that each non-base edge is incident to the outer face of the drawing. The base edge will be drawn horizontally. By the second part of invariant (I1), all vertices not incident to the base edge are above the base edge. Consequently, the base edge is incident to the outer face as well and, hence, the representation is reducible. Finally, by invariant (I4), every vertex belongs to the outer face.

**Construction.** To carry out step (S1), we draw the base edge horizontally and place the stacked vertices on a common horizontal line above the base edge; see Figure 4a. Circular arcs that satisfy the invariants are now easy to define.

Let  $\Gamma$  be a drawing of the graph obtained after step (S1) and some number of iterations of step (S2) such that  $\Gamma$  is equipped with a set of circular arcs satisfying the invariants (I1)–(I4). We describe how to carry out another iteration of step (S2) while maintaining the invariants.

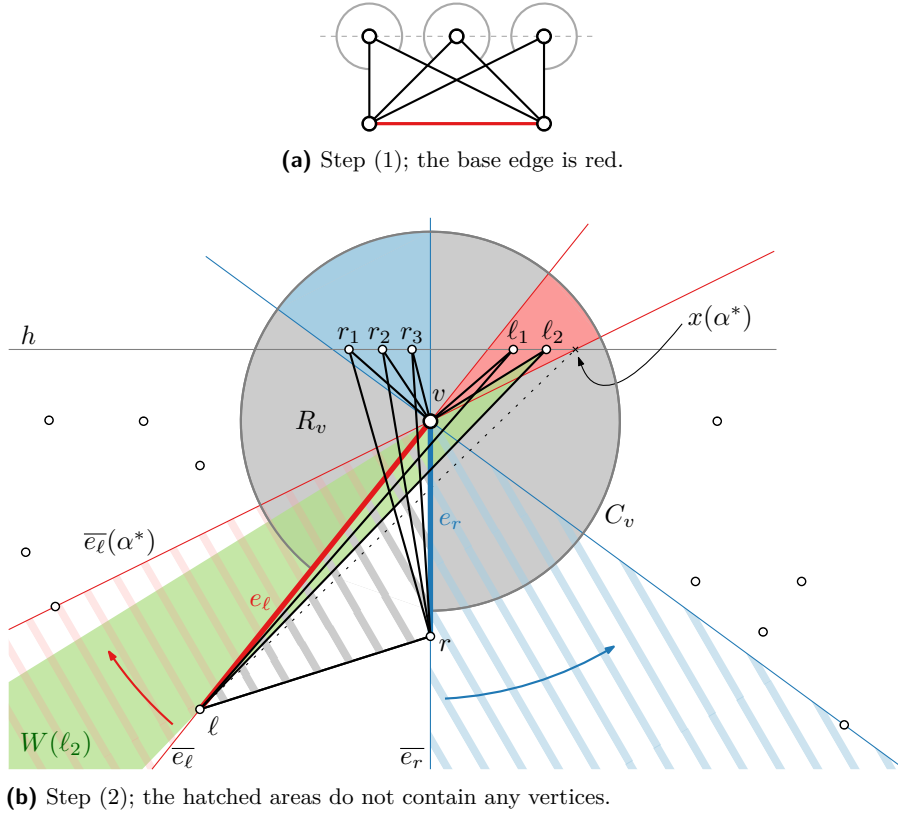
Let  $v$  be an active vertex. By invariant (I1), both parent edges of  $v$  are below  $v$ . Let  $e_\ell = vl$  and  $e_r = vr$  be the left and the right parent edges of  $v$ , respectively. Let  $\ell_1, \ell_2, \dots, \ell_i$  and  $r_1, r_2, \dots, r_j$  be the vertices stacked onto  $e_\ell$  and  $e_r$ , respectively. We refer to  $\ell_1, \ell_2, \dots, \ell_i$  and  $r_1, r_2, \dots, r_j$  as the *new* vertices; the vertices of  $\Gamma$  are called *old*. See Figure 4b for the following construction details. We place all the new vertices on a common horizontal line  $h$  that intersects  $R_v$  above  $v$ . The vertices  $\ell_1, \ell_2, \dots, \ell_i$  are placed inside  $R_v$ , to the right of the line  $\overline{e_\ell}$  extending  $e_\ell$ . Symmetrically,  $r_1, r_2, \dots, r_j$  are placed inside  $R_v$ , to the left of the line  $\overline{e_r}$  extending  $e_r$ . For  $k \in \{1, 2, \dots, i\}$ , let  $W(\ell_k)$  be the smallest open wedge with apex  $\ell_k$  that contains  $e_\ell$ . For example, in Figure 4b, the green shaded wedge is  $W(\ell_2)$ . Note that  $W(\ell_k)$  is bounded by the two rays that go from  $\ell_k$  through  $v$  and through  $\ell$ . For  $k \in \{1, 2, \dots, j\}$ , let  $W(r_k)$  be defined symmetrically.

We place  $\ell_1, \ell_2, \dots, \ell_i$  close enough to  $\overline{e_\ell}$  and  $r_1, r_2, \dots, r_j$  close enough to  $\overline{e_r}$  such that the following properties are satisfied:

(A) None of the parent edges of the new vertices intersects  $C_v$ .

(B) For each new vertex  $y$ , the wedge  $W(y)$  does not contain any vertices of  $T$ .

These properties are easy to achieve: let  $\overline{e_\ell}(\alpha)$  be the line that is obtained by rotating  $\overline{e_\ell}$  clockwise around  $v$  by angle  $\alpha$ . Clearly, there is an angle  $\alpha^*$  such that



■ **Figure 4** Construction steps in the proof of Theorem 2.

(A') the intersection point  $x(\alpha^*)$  of  $\overline{e_\ell}(\alpha^*)$  and  $h$  lies in  $R_v$ , the line segment  $\overline{x(\alpha^*)\ell}$  does not intersect  $C_v$ , and

(B') the unbounded wedge with apex  $v$  (hatched in red in Figure 4b) that goes from  $\overline{e_\ell}$  to  $\overline{e_\ell}(\alpha^*)$  in clockwise direction contains no vertices.

We place the vertices  $\ell_1, \ell_2, \dots, \ell_i$  between  $\overline{e_\ell}$  and  $x(\alpha^*)$ . Then property (A') guarantees property (A). Similarly, property (B') and invariants (I3) and (I4) for  $\Gamma$  imply property (B). The vertices  $r_1, r_2, \dots, r_j$  are placed symmetrically by rotating  $\overline{e_r}$  around  $v$  counterclockwise.

**Correctness.** We now show that the invariants are maintained during the construction. By invariant (I3), for each old vertex  $v$ , the region  $R_v$  is completely contained in the outer face of  $\Gamma$ . Hence, it is easy to define circular arcs for the new vertices that satisfy invariant (I1). To show that invariant (I1) also holds for the circular arcs of the old vertices, we argue as follows. By property (A) of the construction, the parent edge  $e$  of a new vertex  $v$  can be decomposed as follows: a line segment  $e_1$  that lies in  $R_v$  and a line segment  $e_2$  that lies in the triangle  $\triangle \ell r v$  formed by the endpoints of the parent edges of  $v$  (hatched in gray in Figure 4b).

By invariant (I3) for  $\Gamma$ , the region  $R_v$  is empty and, hence,  $e_1$  does not intersect the circular arc of any old vertex. By invariant (I1) for  $\Gamma$ , the circular arcs of the old vertices lie in the outer face of  $\Gamma$  and, hence, it follows that  $e_2$  also does not intersect the circular arc of any old vertex. Consequently, invariant (I1) is maintained for the circular arcs of old vertices.

Invariant (I2) is retained for the non-edges that join two old vertices since the circular arcs of these vertices have not been changed. Property (B) and the fact that all new vertices

are placed on  $h$  imply that each of the non-edges incident to a new vertex  $w$  intersect  $C_w$ . Hence, invariant (I2) is also satisfied for the new non-edges.

Invariant (I3) holds for the circular arcs of the new vertices by invariant (I3) for  $v$  in  $\Gamma$  and by (I1) for the new vertices. To see that invariant (I3) holds for the circular arcs of the old vertices, let  $u \neq v$  be an old vertex. Let  $e$  be a parent edge of a new vertex and recall the definitions of  $e_1$  and  $e_2$  from above. The part  $e_1$  lies in  $R_v$  and  $e_2$  does not pass through the outer face of  $\Gamma$ . Hence, it follows that invariant (I3) is retained for  $u$ .

By invariant (I3) for  $\Gamma$ , the region  $R_v$  is contained in the outer face of  $\Gamma$ . Hence, by construction, invariant (I4) holds for  $v$  and the new vertices. Moreover, invariant (I4) is also retained for the remaining vertices since, by construction, the edges incident to new vertices intersect the outer face of  $\Gamma$  in  $R_v$  only. ◀

### 3 Convex Outside Obstacle Representations

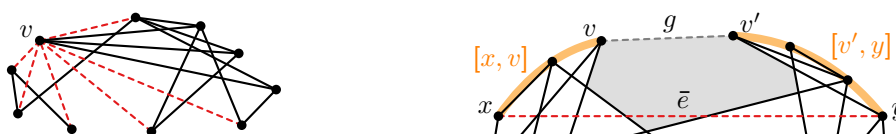
In this section we introduce a sufficient condition and a necessary condition for a graph to admit a convex OOR and then use these conditions to characterize the complements of trees and cycles that admit convex OORs.

We start with the sufficient condition. Suppose that a graph  $G$  admits a convex OOR  $\Gamma$ . Let  $\sigma$  be the clockwise cyclic order of the vertices of  $G$  along the convex hull of  $\Gamma$ . If all neighbors of a vertex  $v$  of  $G$  are consecutive in  $\sigma$ , we say that  $v$  has the *consecutive-neighbors property*, which implies that all non-edges incident to  $v$  are consecutive around  $v$  and trivially intersect the outer face in the immediate vicinity of  $v$ ; see Figure 5a. Note that this combinatorial condition is independent of the exact location of the vertices as long as they are in convex position and their clockwise order is fix. This yields the following result.

► **Lemma 3** (Consecutive-neighbors property). *Let  $G$  be a graph, and let  $\sigma$  be a cyclic order of  $V(G)$ . If there is a subset  $V'$  of  $V(G)$  such that*

- every non-edge of  $G$  is incident to a vertex in  $V'$  and
- every vertex in  $V'$  has the consecutive-neighbors property with respect to  $\sigma$ ,

*then  $G$  admits a convex OOR with cyclic vertex order  $\sigma$  on any set of points in convex position.*

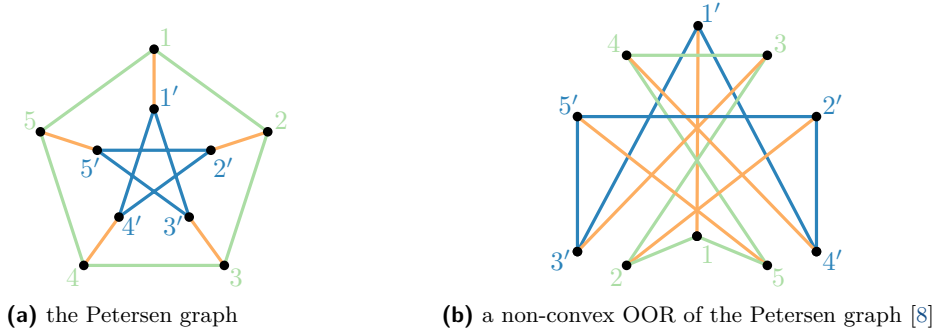


(a) Vertex  $v$  has the consecutive-neighbors property. (b) Gap  $g$  is a candidate gap for the non-edge  $\bar{e}$ .

■ **Figure 5** Examples for (a) the consecutive-neighbors property and (b) a candidate gap.

If a graph  $G$  fulfills the condition stated in the above lemma, then we say that  $G$  has the *consecutive-neighbors property*. Note that the consecutive-neighbors property is not a necessary condition for a graph to admit a convex OOR. For example, we will show that every grid graph admits a convex (even a regular) OOR (Theorem 8), but the OORs that we construct do not fulfill the consecutive-neighbors property (see, for example, vertex  $s$  in Figure 14).

Next, we derive the necessary condition. For any two consecutive vertices  $v$  and  $v'$  in  $\sigma$  that are not adjacent in  $G$ , we say that the line segment  $g = \overline{vv'}$  is a *gap*. Then the *gap region* of  $g$  is the inner face of  $\Gamma + vv'$  incident to  $g$ ; see the gray region in Figure 5b. We



■ **Figure 6** The Petersen graph does not admit a convex OOR.

consider the gap region to be open, but add to it the relative interior of the line segment  $\overline{vv'}$ , so that the non-edge  $vv'$  intersects its own gap region. Observe that each non-edge  $\bar{e} = xy$  that intersects the outer face has to intersect some gap region in an OOR. Suppose that  $g$  lies between  $x$  and  $y$  with respect to  $\sigma$ , that is,  $[v, v'] \subseteq [x, y]$ . We say that  $g$  is a *candidate gap* for  $\bar{e}$  if there is no edge that connects a vertex in  $[x, v]$  and a vertex in  $[v', y]$ . (In Figure 5b, the two intervals are highlighted in orange.) Note that  $\bar{e}$  can intersect only gap regions of candidate gaps.

► **Lemma 4** (Gap condition). *A graph  $G$  admits a convex OOR with cyclic vertex order  $\sigma$  only if, for every non-edge of  $G$ , there exists a candidate gap with respect to  $\sigma$ .*

It remains an open problem whether the gap condition is also sufficient. Nonetheless, we can use the gap condition for no-certificates. To this end, we derived a SAT formula from the following expression, which checks the gap condition for every non-edge of a graph  $G$ :

$$\bigwedge_{xy \notin E(G)} \left[ \bigvee_{v \in [x, y]} \left( \bigwedge_{u \in [x, v], w \in (v, y]} uw \notin E(G) \right) \vee \bigvee_{v \in [y, x]} \left( \bigwedge_{u \in [y, v], w \in (v, x]} uw \notin E(G) \right) \right]$$

We have used this formula to test whether all connected cubic graphs with up to 16 vertices admit convex OORs. The only counterexample that we found was the Petersen graph; see Figure 6. The so-called Blanuša snarks, the Pappus graph, the dodecahedron, and the generalized Peterson graph  $G(11, 2)$  satisfy the gap condition. The latter three graphs do admit convex OORs [8].

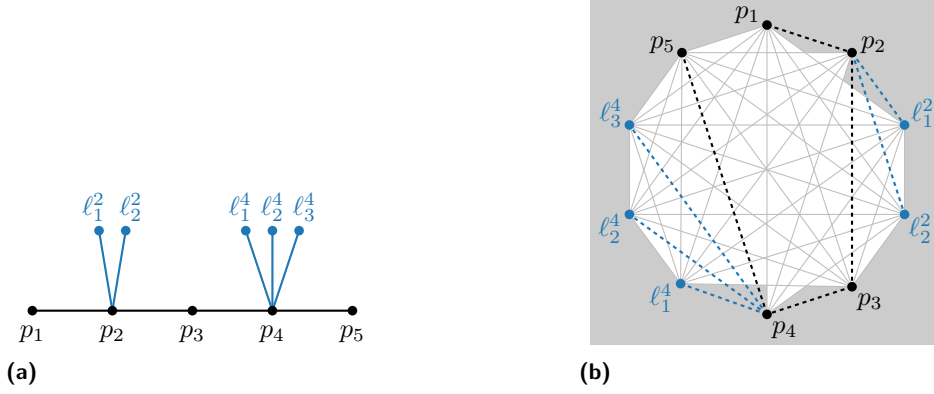
The smallest graph (and the only 6-vertex graph) that does not satisfy the gap condition is the wheel graph  $W_6$  (see Proposition 11 in Section 5). Hence,  $W_6$  does not admit a *convex* OOR, but it does admit a (non-convex) OOR; see Figure 2a.

Next, we turn to dense graphs.

**Complement of a Tree.** For a graph  $G$ , the graph  $\bar{G}$  with  $V(\bar{G}) = V(G)$  and  $\bar{E}(G) = \{uv : uv \notin E(G)\}$  is the *complement* of  $G$ . A *caterpillar* is a tree that contains a path such that all vertices are at distance at most 1 from the path.

► **Theorem 5.** *For any tree  $T$ , the graph  $\bar{T}$  has a convex OOR if and only if  $T$  is a caterpillar.*

**Proof.** We prove the statement in two steps. First, we show that, for every caterpillar  $C$ , the graph  $\bar{C}$  has a convex OOR, in fact, a regular OOR. Then we show that, for every tree  $T$  that is not a caterpillar,  $\bar{T}$  does not admit any convex OOR.



■ **Figure 7** A caterpillar and a regular OOR of its complement.

Let  $C$  be a caterpillar, and let  $\Pi = \langle p_1, p_2, \dots, p_r \rangle$  be a path in  $C$  such that every vertex in  $C$  has distance at most 1 from this path and such that  $p_1$  and  $p_r$  are vertices of degree 1 in  $C$ ; see Figure 7a for an example. For  $i \in \{2, \dots, r-1\}$ , let  $\ell_1^i, \ell_2^i, \dots, \ell_{n_i}^i$  be the leaves adjacent to path vertex  $p_i$  (if any). We arrange the vertices of  $\bar{C}$  in cyclic order as follows. First, we take the path vertices in the given order. Then, for each  $i \in \{2, \dots, r-1\}$ , we insert the leaves adjacent to vertex  $p_i$  between  $p_i$  and  $p_{i+1}$  into the cyclic order; see Figure 7b.

The resulting cyclic order is  $\sigma = \langle p_1, p_2, \ell_1^2, \ell_2^2, \dots, \ell_{n_2}^2, \dots, p_{r-1}, \ell_1^{r-1}, \ell_2^{r-1}, \dots, \ell_{n_{r-1}}^{r-1}, p_r \rangle$ . Observe that every non-edge of  $\bar{C}$  is incident to a vertex in  $V(\Pi)$  and that, for every  $i \in \{2, \dots, r\}$ , vertex  $p_i$  in  $V(\Pi)$  has the consecutive-neighbors property with respect to  $\sigma$  if we view its “incoming” non-edge from  $p_{i-1}$  as an edge. We may do this since this non-edge is still viewed as a non-edge from its other endpoint. Note that  $p_1$  trivially has the consecutive-neighbors property. Hence, by Lemma 3,  $\bar{C}$  admits a convex OOR with cyclic vertex order  $\sigma$  on any set of points in convex position, that is,  $\bar{C}$  admits even a regular OOR.

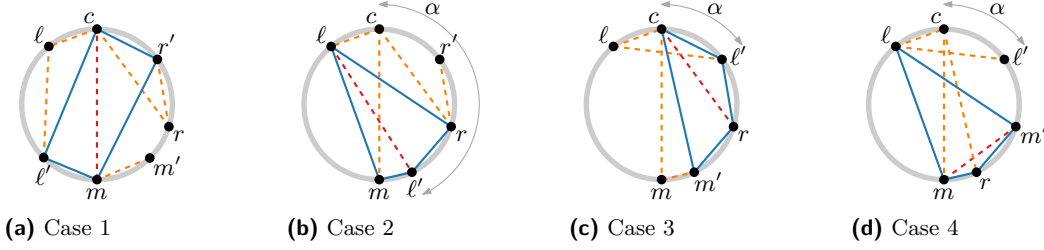
Now we prove the second part of the statement. Let  $Y$  be the tree that consists of a root  $c$  with three children  $\ell$ ,  $m$ , and  $r$ , each of which has one child, namely  $\ell'$ ,  $m'$ , and  $r'$ , respectively; see Figure 8a. Let  $T$  be a tree that is not a caterpillar. Note that  $T$  has a subtree that is isomorphic to  $Y$ .

Let  $\sigma$  be any cyclic order of  $V(Y)$ . We now show that  $\bar{T}$  admits no convex OOR with respect to  $\sigma$ . To this end, we find an edge  $e$  of  $Y$  (i.e., a non-edge of  $\bar{T}$ ) that is a diagonal of a convex quadrilateral  $Q$  formed by four non-edges of  $Y$ . Observe that any non-edge of  $Y$  must be an edge of  $\bar{T}$  (otherwise  $T$  would contain a cycle). Hence, the non-edge  $e$  of  $\bar{T}$  (being enclosed by a 4-cycle of edges of  $\bar{T}$ ) does not have a candidate gap, which by Lemma 4 implies that  $\bar{T}$  does not admit a convex OOR.

It remains to show the existence of  $e$  and  $Q$ . Without loss of generality, let  $\langle c, r, m, \ell \rangle$  be the order of  $c$  and its children in  $\sigma$ . We distinguish four cases.



■ **Figure 8** (a) The smallest tree  $Y$  that is not a caterpillar and (b) a non-convex OOR of  $\bar{Y}$ .



■ **Figure 9** Case distinction in the proof of Theorem 5: (a) Case 1:  $cm$  is not intersected; (b) Case 2:  $ll'$  intersects  $cm$ ,  $\alpha \cap Y \neq \emptyset$ ; (c) Case 3:  $ll'$  intersects  $cm$ ,  $\alpha \cap Y = \emptyset$ , and  $c, r, m'$  appear in this order in  $\sigma$ ; (d) Case 4: otherwise.

**Case 1:** None of the edges of  $Y$  intersects  $cm$ ; see Figure 9a.

Then  $e = cm$  lies inside the quadrilateral  $Q = \langle c, r', m, \ell' \rangle$  formed by non-edges of  $Y$ . In the following three cases, we assume, without loss of generality, that  $ll'$  intersects  $cm$ . Let  $\alpha$  be the open circular arc from  $c$  to  $\ell'$  in clockwise direction.

**Case 2:**  $\alpha \cap Y \neq \emptyset$ , i.e., at least one vertex of  $Y$  lies in  $\alpha$ , say  $r$ ; see Figure 9b.

Then  $e = \ell\ell'$  lies inside the quadrilateral  $Q = \langle \ell, r, \ell', m \rangle$ .

In the remaining two cases, we assume that  $\alpha \cap Y = \emptyset$ .

**Case 3:** The vertices  $c, r$ , and  $m'$  appear in this order in  $\sigma$ ; see Figure 9c.

Then  $e = cr$  lies inside the quadrilateral  $Q = \langle c, \ell', r, m' \rangle$ .

**Case 4:** Otherwise; see Figure 9d.

Then  $e = mm'$  lies inside the quadrilateral  $Q = \langle \ell, m', r, m \rangle$ .

To conclude,  $e$  and  $Q$  always exist. ◀

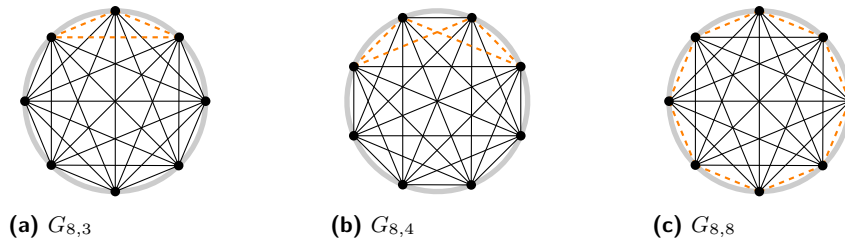
Figure 8a depicts the smallest tree  $Y$  that is not a caterpillar and, hence, its complement  $\bar{Y}$  does not admit a convex OOR. The graph  $\bar{Y}$  does, however, admit an OOR; see Figure 8b.

**Complete Graph Minus a Cycle.** Using the gap condition (Lemma 4), we can prove the following theorem in a similar way as Theorem 5. Let  $C_k$  be a simple cycle of length  $k$ .

► **Theorem 6.** *Let  $3 \leq k \leq n$ . Then the graph  $G_{n,k} = K_n - E(C_k)$  admits a convex OOR if and only if  $k \in \{3, 4, n\}$ .*

**Proof.** First, we show that, for  $k \in \{3, 4, n\}$ , the graph  $G_{n,k}$  admits a convex OOR. To this end, we place the vertices  $v_1, \dots, v_k$  of  $C_k$  as an interval on a circle. If  $k < n$ , we place the remaining vertices in an arbitrary order, also as an interval, on the same circle. For  $k = 3$ , the vertex order of  $C_3$  is determined; see Figure 10a. For  $k = 4$ , we place the vertices of  $C_4$  in the order  $\langle v_1, v_2, v_4, v_3 \rangle$ ; see Figure 10b. For  $k = n$ , we take the vertex order of  $C_n$ ; see Figure 10c. In the cases  $k = 3$  and  $k = n$ , let  $V' = V(G_{n,k})$ . In the case  $k = 4$ , let  $V' = V(G_{n,k}) \setminus \{v_2, v_4\}$  and note that  $v_2$  and  $v_4$  are adjacent in  $G_{n,k}$ . In all cases all vertices in  $V'$  satisfy the consecutive-neighbors property and  $V'$  covers all non-edges. Therefore, by Lemma 3, the graph  $G_{n,k}$  admits a convex OOR with respect to the cyclic vertex order (depending on  $k$ ) described above. Note that, in all cases, we fixed only the cyclic order of vertices and not their specific position. Thus, we can obtain the regular OORs.

Now let  $k \in \{5, \dots, n-1\}$ . The graph  $G_{n,k}$  contains at least one vertex  $v$  that is adjacent to all other vertices. Let  $\sigma$  be any cyclic order of  $V(G_{n,k})$  starting at  $v$  in clockwise direction. We prove that  $G_{n,k}$  does not admit a convex OOR with respect to  $\sigma$ . To this end, let  $c$  be



■ **Figure 10** Regular OORs of the graph  $G_{n,k}$  for  $n = 8$  and (a)  $k = 3$ , (b)  $k = 4$ , (c)  $k = n$ .

the first vertex of  $C_k$  after  $v$  in  $\sigma$ . Let  $c'$  be the last vertex in  $\sigma$  that is not adjacent to  $c$ . We consider two cases.

**Case 1:** There is only one vertex  $m$  of  $C_k$  in the interval  $(c, c')$ ; see Figure 11a.

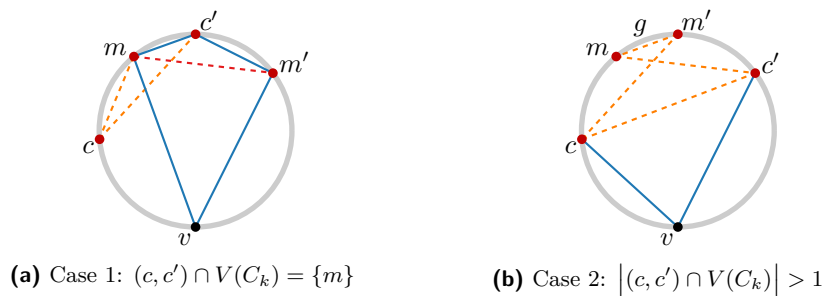
Note that  $cm$  is a non-edge. Let  $m'$  be the other vertex that shares a non-edge with  $m$ . Note that  $m'$  lies between  $c'$  and  $v$  since  $c$  is the first vertex of  $C_k$  after  $v$ . Hence,  $mm'$  is a diagonal of the quadrilateral  $Q = \langle v, m, c', m' \rangle$ . We argue that the edges of  $Q$  belong to  $G_{n,k}$ . By the choice of  $v$ , this is the case for  $vm$  and  $vm'$ . The same holds true also for  $mc'$  and  $c'm'$ , otherwise the non-edges of  $G_{n,k}$  would contain a  $C_3$  or a  $C_4$ , respectively. However,  $G_{n,k}$  has a simple  $k$ -cycle of non-edges with  $k \geq 5$ .

**Case 2:** There are at least two vertices of  $C_k$  in the interval  $(c, c')$ ; see Figure 11b.

Recall that  $cc'$  is a non-edge of  $G_{n,k}$ . For  $G_{n,k}$  to admit a convex OOR with respect to  $\sigma$ , by Lemma 4,  $cc'$  would have to have a candidate gap  $g$ , i.e., an edge  $mm'$  of  $C_k$ . Due to the presence of the edges  $vc$  and  $vc'$ , the gap  $g$  must lie on the side of  $cc'$  opposite of  $v$ . By the definition of a candidate gap, no edge connects the intervals  $[c, m]$  and  $[m', c']$ . This implies that  $cm'$  and  $mc'$  are non-edges. Hence,  $\langle c, c', m, m' \rangle$  is a 4-cycle of non-edges – a contradiction to the fact that  $G_{n,k}$  has a simple  $k$ -cycle of non-edges only with  $k \geq 5$ . In both cases, we have that  $G_{n,k}$  does not admit a convex OOR with respect to  $\sigma$ . ◀

#### 4 Regular Outside Obstacle Representations

This section deals with regular OORs of three graph classes. A *cactus* is a connected graph where every edge is contained in at most one simple cycle. The *weak dual* of a plane graph or a planar drawing is its dual graph without the vertex corresponding to the outer face. An *outerpath* is a graph that admits an *outerpath* drawing, i.e., an outerplanar drawing whose weak dual is a path. Let  $P_k = \langle v_1, \dots, v_k \rangle$  denote a (simple) path with  $k$  vertices. A graph  $G$  is a *grid graph* (or simply a grid) if there are positive integers  $k$  and  $\ell$  such that  $G = P_k \square P_\ell$ ,



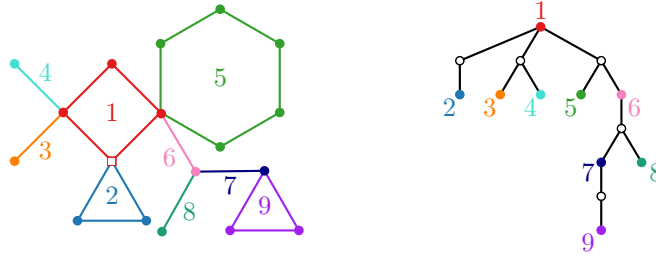
■ **Figure 11** Case distinction in the proof of Theorem 6.

that is, if  $V(G) = V(P_k) \times V(P_\ell)$  and if  $G$  contains an edge between two vertices  $(v_i, v_j)$  and  $(v_{i'}, v_{j'})$  if and only if  $|i - i'| = 0$  and  $|j - j'| = 1$  or vice versa.

► **Theorem 7.** *Every cactus has a reducible regular OOR.*

**Proof.** For the given cactus  $G$ , we first compute the block-cut tree (whose definition we recall below). Then, following the structure of the block-cut tree, we treat the blocks one by one. For each block, we insert its vertices as an interval into the vertex order of the subgraph that we have treated so far. Finally, we prove that the resulting cyclic vertex order yields a reducible regular OOR.

A *block-cut tree* of a connected graph is a tree that has a vertex for each cut vertex and for each *block*, which can either be a maximal biconnected subgraph or a bridge (cut edge). There is an edge in the block-cut tree for each pair  $(B, v)$  of a block  $B$  and a cut vertex  $v$  with  $v \in V(B)$ . For an example of a block-cut tree of a cactus, see Figure 12. We root the block-cut tree in an arbitrary block vertex and number the block vertices according to a breadth-first search traversal starting at the root.



■ **Figure 12** A cactus and its block-cut tree. White tree nodes correspond to cut vertices in the cactus.

In order to draw the cactus  $G$ , we treat its blocks one by one and insert the vertices of each block into the cyclic order, starting with the root block. For each further block  $B$ , there is a cut vertex  $v_B \in V(B) \cap V(B')$  where  $B'$  is a block that we have treated earlier. We insert the vertices of  $B$  as an interval between  $v_B$  and its clockwise successor in the current cyclic vertex order. For the root block  $B^*$ , let  $v_{B^*}$  be an arbitrary vertex of  $B^*$  (marked by a white square in Figures 12 and 13).

Now we draw the current block  $B$ . If  $B$  is a single edge  $v_B w$ , we place  $w$  immediately behind  $v_B$ . If  $B$  is a cycle with  $k$  vertices ( $k \geq 3$ ), we start with the cut vertex  $v_B$  and proceed in a zig-zag manner, mapping the vertices to positions 1 (which is  $v_B$ ),  $k, 2, k-1, \dots, \lceil (k+1)/2 \rceil$ ; see Figure 13 (center). For  $k \leq 4$ , all vertices of  $B$  satisfy the consecutive-neighbors property. For  $k \geq 5$ , exactly two vertices do not satisfy this property, but these two vertices are adjacent, so by Lemma 3 all non-edges of  $B$  intersect the outer face as required.

Now we draw  $G$  by placing the vertices in the cyclic order on a circle that we just defined; the exact positions on the circle do not matter. Consider the convex hulls of the blocks in the drawing. Observe that any two of them share at most one vertex. Moreover, the boundary of each convex hull lies completely in the outer face of the drawing. In the process described above, each block has its own OOR due to Lemma 3. Hence, the whole drawing is an OOR of  $G$ . The representation is reducible since each vertex has degree at most 2 within each block, and each block is surrounded by the outer face.

Since only the order of the vertices along the circle is important for the OOR, not their exact positions, it is easy to obtain a regular OOR. For the same reason, even cactus forests admit OORs. ◀

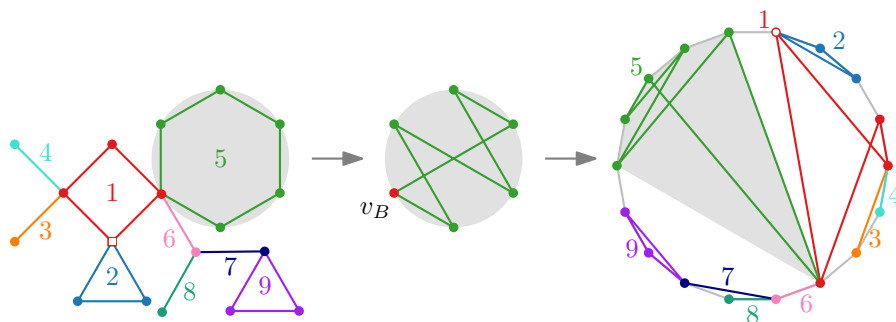


Figure 13 Constructing a reducible regular OOR of a cactus.

► **Theorem 8.** *Every grid has a reducible regular OOR.*

**Proof.** Let  $k$  and  $\ell$  be positive integers such that the grid is  $G = P_k \square P_\ell$ . We name the vertices of  $P_k$  such that  $P_k = \langle v_1, \dots, v_k \rangle$ . We assume that  $k \geq \ell$ . We place the vertices of each copy of  $P_k$  in a zig-zag manner on consecutive corners of a regular  $k\ell$ -gon, that is, in the order  $v_k, v_{k-2}, v_{k-4}, \dots, v_5, v_3, v_1, v_2, v_4, \dots, v_{k-1}$  if  $k$  is odd and in the order  $v_k, v_{k-2}, v_{k-4}, \dots, v_4, v_2, v_1, v_3, v_5, \dots, v_{k-1}$  if  $k$  is even; see Figure 14. If  $\ell = 1$ , then  $G$  is a path and the zig-zag order that we just described defines a regular OOR, hence we may assume that  $\ell \geq 2$  from now on. The copies of  $P_k$  (black in Figure 14) are placed directly one after the other. This fixes our drawing of  $G$ .

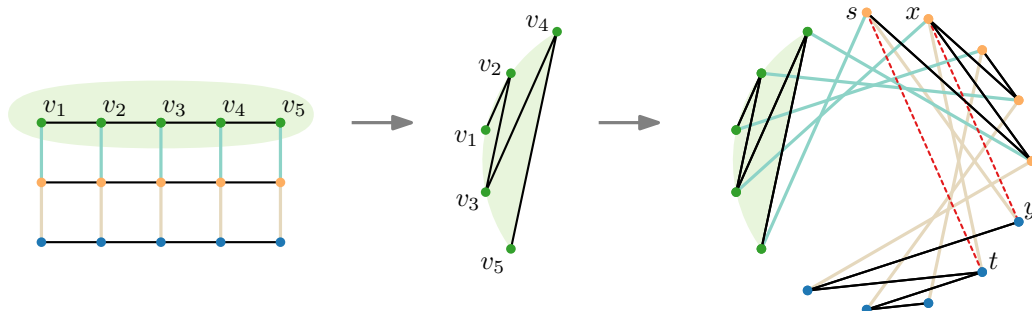
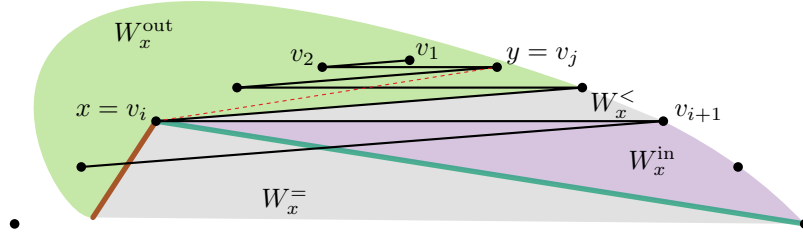


Figure 14 Constructing a reducible regular OOR of the grid  $P_5 \square P_3$ .

Given a pair  $\{s, t\}$  of vertices of  $G$ , we say that the *cyclic length* of the edge or non-edge  $st$  is  $d$  if the line through  $s$  and  $t$  splits the plane into two open halfplanes such that the one that contains fewer vertices of  $G$  contains exactly  $d - 1$  vertices. Within  $P_k$ , the longest edge is  $v_{k-1}v_k$ ; it has cyclic length  $k - 1$ . Since the copies of  $P_k$  are placed directly one after the other, every edge within a copy of  $P_\ell$  (colored lightly in Figure 14) has cyclic length exactly  $k$ .

We now show that every non-edge intersects the outer face. First, consider a non-edge  $st$  that has cyclic length at least  $k + 1$ ; see Figure 14. Then it is longer than every edge of  $G$ ; hence it intersects the gap region  $g$  between the first and the last copy of  $P_k$ . Note that non-edges of length exactly  $k$  exist only between vertices of the first and the last copy of  $P_k$ , but these non-edges, too, intersect the gap region  $g$ .

Next, consider a non-edge  $xy$  that has length less than  $k$ . As every vertex of  $G$ ,  $x$  is incident to one or two edges of length  $k$  (contained in a copy of  $P_\ell$ ) and to one or two edges of length less than  $k$  (contained in a copy of  $P_k$ ). Let  $W_x^-$  be the wedge with apex  $x$  formed



■ **Figure 15** The four wedges with respect to a vertex  $x$  of the grid graph  $P_k \square P_\ell$ . The black edges represent a copy of  $P_k$ . The two colored edges of length  $k$  belong to the same copy of  $P_\ell$ .

by (and including) the length- $k$  edge(s) – if there is just one such edge, then  $W_x^=$  is the ray starting in  $x$  that contains this edge; see Figure 15. Similarly, let  $W_x^<$  be the wedge formed by (and including) the shorter edge(s). Hence, the angular space around  $x$  is subdivided into four wedges:  $W_x^=$ ,  $W_x^<$ ,  $W_x^{in}$ , and  $W_x^{out}$ , where  $W_x^{out}$  is the (open) wedge between  $W_x^=$  and  $W_x^<$  that intersects the outer face of the drawing in the vicinity of  $x$ , and  $W_x^{in}$  is the remainder of the plane. Let  $W_y^=$ ,  $W_y^<$ ,  $W_y^{in}$ , and  $W_y^{out}$  be defined analogously with respect to  $y$ . Note that the line segment  $\overline{xy}$  is neither contained in  $W_x^=$  nor in  $W_x^<$ . This is due to the fact that  $W_x^=$  contains only vertices of distance greater than  $k$  and  $W_x^<$  contains no vertices in its interior. For the same reasons,  $\overline{xy}$  is neither contained in  $W_y^=$  nor in  $W_y^<$ . We now show that  $\overline{xy}$  lies in  $W_x^{out}$  or in  $W_y^{out}$ , which implies that  $\overline{xy}$  intersects the outer face of the drawing in the vicinity of  $x$  or  $y$ , respectively. We consider two cases.

**Case 1:** Vertex  $y$  belongs to the same copy of  $P_k$  as  $x$ .

Let  $i, j \in \{1, \dots, k\}$  be such that  $x = v_i$  and  $y = v_j$ . First suppose that  $j < i$ ; see Figure 15. Then, by our layout, the cyclic length of  $xy$  is less than  $i$ . The non-edges in  $W_x^{in}$ , however, have cyclic length at least  $i$ . (The edge  $v_i v_{i+1}$  is the shortest edge in  $W_x^{in}$  and has cyclic length  $i$ ; see Figure 15.) Hence,  $\overline{xy}$  cannot lie in  $W_x^{in}$  and must lie in  $W_x^{out}$ . If  $j > i$ , we can argue analogously (by swapping  $x$  with  $y$  and  $i$  with  $j$ ) to show that  $\overline{xy}$  lies in  $W_y^{out}$ .

**Case 2:** Vertex  $y$  lies in a different (but neighboring) copy of  $P_k$ , say, the next copy; see Figure 14 (right).

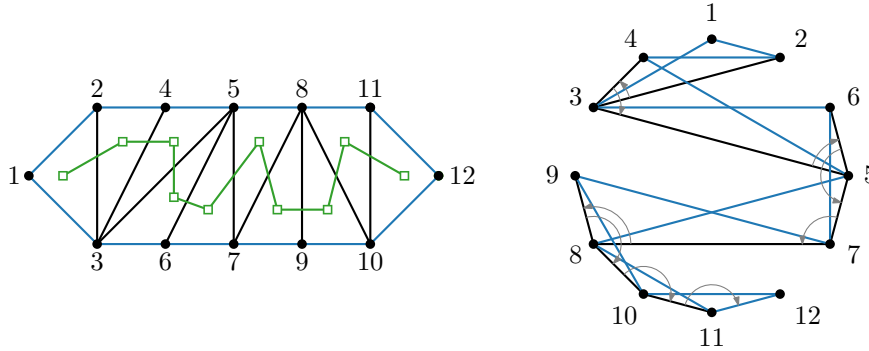
If  $\overline{xy}$  lies in  $W_x^{out}$ , we are done. So suppose that  $\overline{xy}$  lies in  $W_x^{in}$ . This implies that  $x$  must lie in the first half (that is,  $x \in \{v_k, v_{k-2}, \dots, v_1\}$ ) of its copy. Since the cyclic length of  $xy$  is less than  $k$ ,  $y$  must lie in the first half of its copy, too. Due to our layout of  $P_k$ , the (short) edges in  $W_y^<$  go to the other half of the copy. Therefore, the length- $k$  edges that define  $W_y^=$  must lie between the short non-edge  $\overline{xy}$  and the short edges that define  $W_y^<$ . In other words,  $\overline{xy}$  lies in  $W_y^{out}$ .

For reducibility, we can argue similarly as for the non-edges. Indeed, every edge of cyclic length  $k$  is incident to the gap region  $g$  between the first and last copy of  $P_k$ ; see Figure 14 (right). The shorter edges alternate in direction, so for  $i \in \{1, \dots, k-1\}$ , the edge  $v_i v_{i+1}$  of  $P_k$  is adjacent to the outer face in the vicinity of vertex  $v_{i+1}$ . ◀

► **Theorem 9.** *Every outerpath has a reducible regular OOR.*

**Proof.** Let  $G$  be an  $n$ -vertex outerpath, and let  $\Gamma$  be an outerpath drawing of  $G$ . We show that  $G$  admits a reducible regular OOR. The statement is trivial for  $n \leq 3$ , so assume otherwise. By reducibility and appropriately triangulating the inner faces of  $\Gamma$ , we may assume without loss of generality that each inner face of  $\Gamma$  is a triangle. Let the path  $\langle t_1, t_2, \dots, t_{n-2} \rangle$

be the weak dual of  $\Gamma$ . Let  $V_i$  denote the set of vertices of  $G$  that are incident to the triangles  $t_1, t_2, \dots, t_i$ . By definition,  $V_1$  contains a vertex  $v_1$  of degree 2. For  $4 \leq i \leq n$ , let  $v_i$  denote the unique vertex in  $V_{i-2} \setminus \bigcup_{j=1}^{i-3} V_j$ , where  $\bigcup_{j=1}^{i-3} V_j = \{v_1, v_2, \dots, v_{i-1}\}$ ; see Figure 16 (left). For  $4 \leq i < n$ , the vertex  $v_i$  is incident to an inner edge  $e_i = v_i v_j$  of  $\Gamma$  such that  $j < i$  and  $v_j$  belongs to the triangle  $t_{i-3}$ . Let  $G_i = G[v_1, v_2, \dots, v_i]$ . We iteratively construct reducible regular OORs  $\Gamma_3, \Gamma_4, \dots, \Gamma_n$  of  $G_3, G_4, \dots, G_n (= G)$ , respectively. We create  $\Gamma_3$  by arbitrarily drawing  $G_3$  on the circle. For  $4 \leq i < n$ , to obtain  $\Gamma_i$  from  $\Gamma_{i-1}$ , we consider the inner edge  $e_i = v_i v_j$  and place  $v_i$  next to  $v_j$  on the circle, avoiding the (empty) arc of the circle that corresponds to  $e_{i-1}$ ; see Figure 16 (right). So if  $v_j$  is incident to multiple inner edges, then the corresponding neighbors of  $v_j$  alternate on the circle. The vertex  $v_n$  is placed next to  $v_{n-1}$ , avoiding the arc that corresponds to  $e_{n-1}$ . (This yields that  $v_n$  has the consecutive neighbors property.) Note that we fixed only the cyclic order of vertices and not their specific position. Thus, we can place the vertices on a regular polygon.

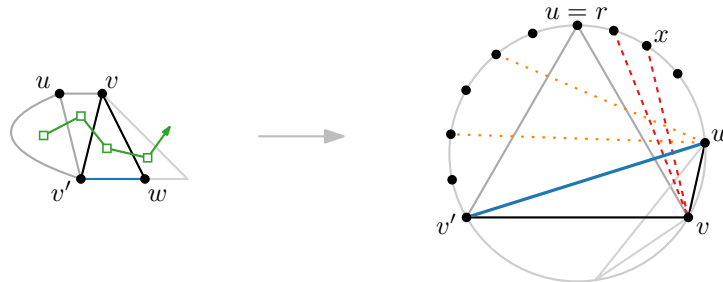


■ **Figure 16** A drawing  $\Gamma$  of an outerpath  $G$  and a reducible regular OOR of  $G$  based on  $\Gamma$ . Inner edges are black, outer edges are blue, weak dual edges are green.

Now we show that each  $\Gamma_i$ , for  $i \in \{3, \dots, n\}$ , is indeed a reducible regular OOR. For any three points  $a, b$ , and  $c$  on the circle  $C$ , let  $h_{ab}^{+c}$  be the open half-plane that is defined by the line  $\ell_{ab}$  through  $a$  and  $b$  and that contains  $c$ . Similarly, let  $h_{ab}^{-c}$  be the open half-plane defined by  $\ell_{ab}$  that does not contain  $c$ . Hence,  $h_{ab}^{+c} \cup \ell_{ab} \cup h_{ab}^{-c} = \mathbb{R}^2$ .

Let  $u, v$ , and  $v'$  be the vertices of the triangle  $t_{i-1}$  with  $i \in \{2, \dots, n-2\}$  such that  $vv'$  is an inner edge. Furthermore, let  $w$  be a new vertex of  $t_i$  and, without loss of generality, let  $vw$  be an inner edge if  $i \neq n-2$ , see Figure 17. By construction of the cyclic order described above, we keep the invariant that when we place  $w$  on  $C$ ,  $h_{vw}^{-u}$  is empty and  $h_{v'w}^{-u}$  contains only  $v$  (among the vertices placed so far).

Now we show that when we add the vertex  $w$ , and, thus, the triangle  $\triangle wv'v$ , a non-edge



■ **Figure 17** Constructing a representation for outerpaths such that the invariants are maintained.

that goes through the outer face of the drawing  $\Gamma_{i-1}$  of  $G_{i-1}$  continues to do so in the drawing  $\Gamma_i$  of  $G_i$ . We assume that  $\Delta wv'v$  is oriented counterclockwise (as in Figure 17). Let  $r$  be the last neighbor of  $v$  in  $G_{i-1}$  in the cyclic order that starts from  $v$  and follows the circle counterclockwise. Since  $u$  is a neighbor of  $v$ ,  $r = u$  (as in Figure 17) or  $r$  lies strictly between  $u$  and  $v$ , but  $r \neq w$  because  $w \notin V(G_{i-1})$ . Note that the half-plane  $h_{v'w}^{-u}$  contains (the interior of)  $\Delta wv'v$ , but  $v$  is the only vertex in  $h_{v'w}^{-u}$ . Therefore, only non-edges incident to  $v$  can be affected by the addition of  $\Delta wv'v$ , and among these only the ones that go through the outer face of  $\Gamma_{i-1}$  in the vicinity of  $v$ . These are the non-edges (dashed red in Figure 17) that are incident to  $v$  and lie in the half-plane  $h_{rv}^{-v'}$  that is induced by  $rv$  and does not contain  $v'$ . Any such non-edge  $vx$  intersects  $v'w$  since  $v$  and  $x$  lie on different sides of  $v'w$ . The intersection point of  $vx$  and  $v'w$  lies on the outer face of  $\Gamma_i$  because  $h_{v'w}^{-u}$  contains only  $v$  and, in  $G_i$ ,  $w$  is incident to only  $v$  and  $v'$ . This proves our claim regarding the “old” non-edges.

The “new” non-edges (dotted orange in Figure 17) are all incident to  $w$  and lie in  $h_{v'w}^{-v}$ . Since the two neighbors of  $w$ , namely  $v$  and  $v'$ , are consecutive in  $\Gamma_i$ , all non-edges incident to  $w$  go through the outer face – at least in the vicinity of  $w$ .

It remains to show that  $\Gamma_i$  is reducible. For the two new edges incident to  $w$  it is clear that they are both part of the outer face – at least in the vicinity of  $w$ . Since  $h_{vw}^{-u}$  is empty, the only old edge that is affected by the addition of  $\Delta wv'v$  is the edge  $vr$ . It used to be part of the outer face at least in the vicinity of  $v$ . Arguing similarly as we did above for the non-edge  $vx$ , we get that the intersection point of  $vr$  and  $v'w$  lies on the outer face. ◀

We consider two further simple graph classes that trivially admit regular OORs. A graph is *convex round* if its vertices can be cyclicly enumerated such that the open neighborhood of every vertex is an interval in the enumeration. A *bipartite graph* with bipartition  $(U, W)$  of the vertex set is *convex* if  $U$  can be enumerated such that, for each vertex in  $W$ , its neighborhood is an interval in the enumeration of  $U$ . Note that every complete bipartite graph is convex. By definition, every convex round and convex bipartite graph admits a cyclic order such that every vertex satisfies the consecutive-neighbors property (Lemma 3). This yields the following.

► **Observation 10.** *Every convex round and convex bipartite graph admits a regular OOR.*

Our representations for convex round graphs, convex bipartite graphs, cacti, outerpaths, and complements of caterpillars rely on the consecutive-neighbors property (Lemma 3). Hence, *any* convex point set of size  $n$  is *universal* in the sense that it can be used as vertex set for an OOR for any graph with  $n$  vertices from one of these families.

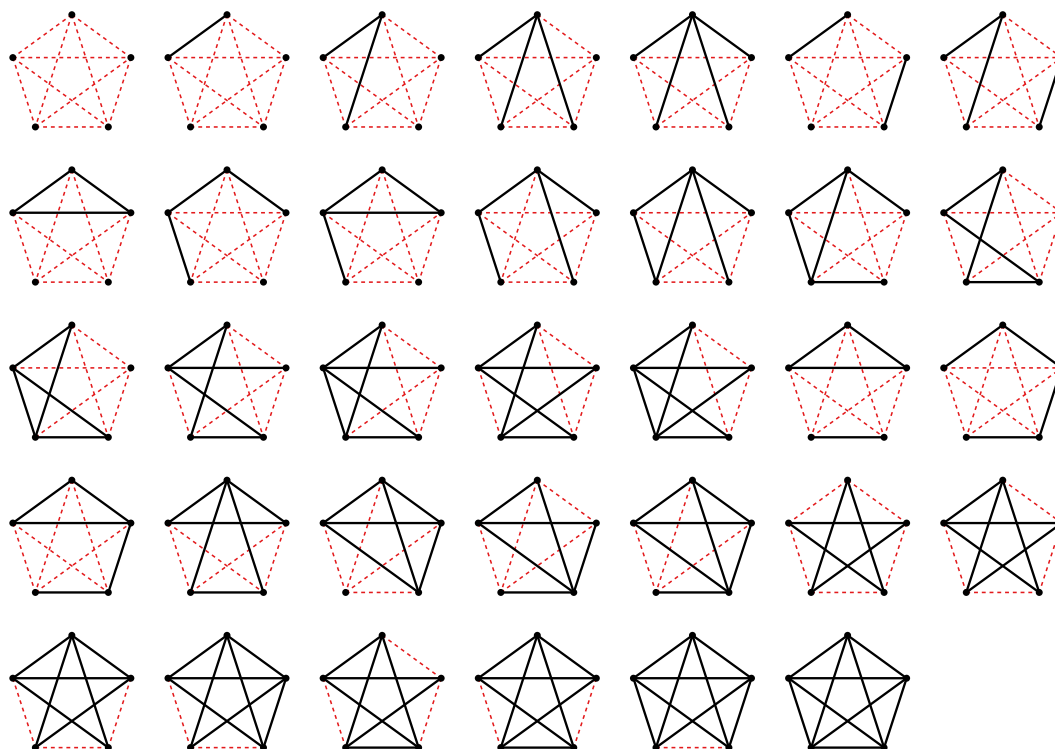
## 5 Small Graphs

In this section we show that every graph with up to six vertices – except for the graph  $W_6$  depicted in Figure 2a – admits a regular OOR (see Proposition 11 below). Lang [9] showed that every outerplanar graph with up to seven vertices admits a regular OOR. The 8-vertex outerplanar graph in Figure 2b, however, does not admit any regular OOR (see Proposition 12 below). It is the only 8-vertex outerplanar graph with this property [9].

► **Proposition 11.** *There exists a regular OOR for every graph with up to six vertices, except for the wheel graph  $W_6$ .*

**Proof.** Note that  $W_6$  is isomorphic to  $G_{6,5} = K_6 - E(C_5)$ . Hence, by Theorem 6,  $W_6$  does not admit a convex OOR. Except for  $G_{6,5}$ , we claim that every graph with at most six

vertices satisfies the gap condition and admits a regular OOR. For graphs with up to four vertices, this is not difficult to check. For graphs with five vertices, see Figure 18.

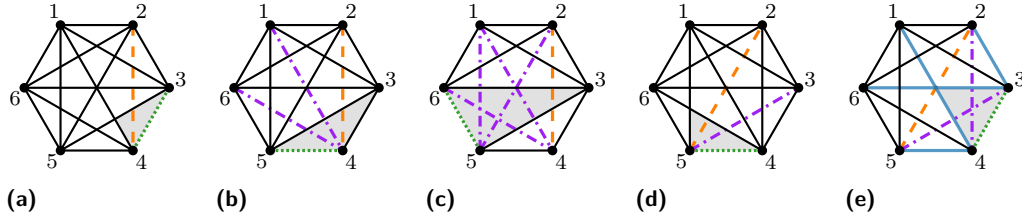


■ **Figure 18** Every graph with up to five vertices admits a regular OOR.

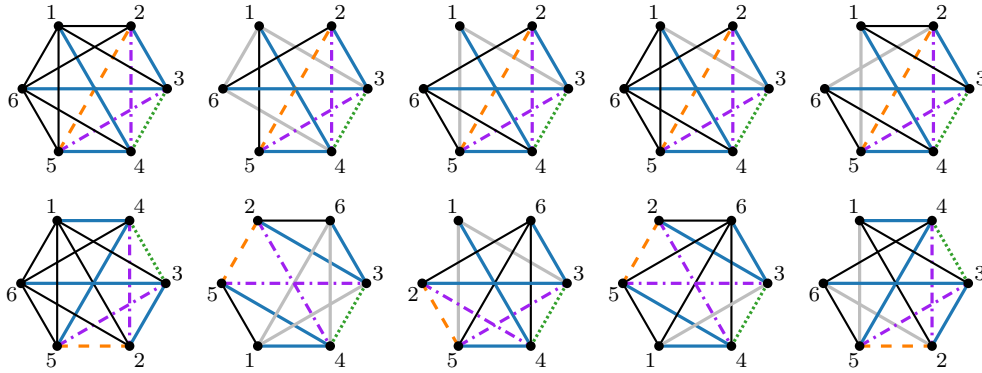
For graphs with six vertices, we used the SAT formulation described in Section 3 to find vertex orders that satisfy the gap condition for the vertex set of the regular hexagon. We now argue that each such vertex order either directly induces a regular OOR or we can find an alternative OOR. To this end, we have to check whether every non-edge intersects a gap region. We do a case distinction depending on the *length* of the non-edges in terms of the number of hexagon edges that they shortcut. There are three cases for a non-edge  $e$  (orange dashed in Figure 19).

- If  $e$  has length 1,  $e$  defines its own gap region, which it intersects.
- If  $e$  has length 2 (see Figures 19a–19c), then there are three possible gaps (up to symmetry, green dotted). For the gap condition to be satisfied for  $e$ , in some cases, there must be further non-edges (purple dash-dotted). In all three cases,  $e$  does intersect a gap region.
- If  $e$  has length 3 (see Figures 19d and 19e), there are two possible gaps (up to symmetry, green dotted). For the situation in Figure 19d, the purple dash-dotted non-edge again makes sure that  $e$  intersects the gap region of the green dotted non-edge. If, however, the endpoints of  $e$  are not incident to the gap (see Figure 19e), then  $e$  may not intersect the gap region of the green dotted non-edge. This is the case if four specific vertex pairs are edges (blue solid). Then  $e$  touches the gap region, but does not intersect it. We analyze this case below.

To solve the remaining case (with blue solid edges  $\{1, 4\}$ ,  $\{2, 3\}$ ,  $\{3, 6\}$ ,  $\{4, 5\}$ ; and orange dashed, green dotted, and purple dash-dotted non-edges  $\{2, 5\}$ ,  $\{3, 4\}$ ,  $\{2, 4\}$ ,  $\{3, 5\}$ , see Figure 19e), we argue that for every graph with this pattern, there exists a vertex order that



■ **Figure 19** Given an orange dashed non-edge  $e$ , there are several (green dotted) candidate non-edges whose gaps could be intersected by  $e$ . Depending on the green dotted candidate non-edge, the existence of additional (purple dash-dotted) non-edges may be necessary to satisfy the gap condition. Due to the blue solid edges, the drawing in (e) is *not* a regular OOR.



■ **Figure 20** The first row depicts sub-cases of the last case from Figure 19; the second row depicts, for each of the upper sub-cases, an alternative vertex order that induces a regular OOR.

does induce a regular OOR. In Figure 20, the first row depicts five cases that cover all possible graphs with the problematic pattern given the original vertex order; the second row depicts a good vertex order for the same graph (where the endpoints of the edge  $\{2, 5\}$  are consecutive). Our case distinction considers every subset  $S$  of the vertex pairs  $\{\{1, 2\}, \{1, 6\}, \{5, 6\}\}$  as non-edges. In each case, the edges (black solid) and the non-edges (non-solid) are enforced by the given case; gray line segments connect vertex pairs that can be either edges or non-edges.

**Case 1:**  $S = \emptyset$  (first column of Figure 20).

**Case 2:**  $S = \{\{1, 2\}, \{5, 6\}\}$  and  $S = \{\{1, 2\}, \{1, 6\}, \{5, 6\}\}$  (second column).

**Case 3:**  $S = \{\{1, 2\}, \{1, 6\}\}$  (third column) and  $S = \{\{1, 6\}, \{5, 6\}\}$  (symmetric).

**Case 4:**  $S = \{\{1, 2\}\}$  (forth column) and  $S = \{\{5, 6\}\}$  (symmetric).

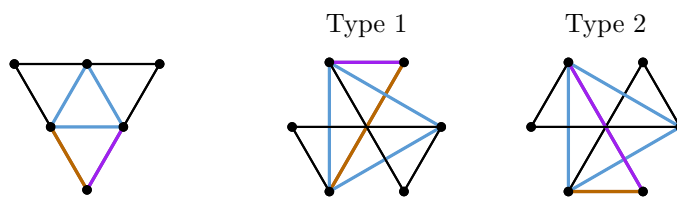
**Case 5:**  $S = \{\{1, 6\}\}$  (fifth column).

This shows that every graph with the problematic pattern admits a regular OOR. ◀

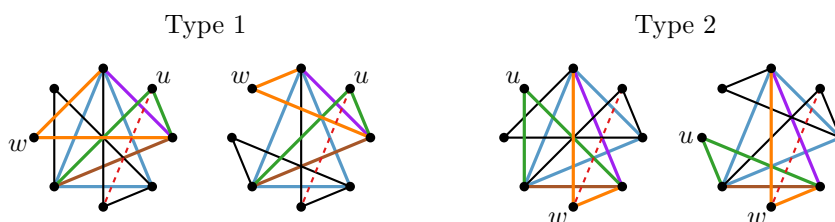
► **Proposition 12.** *There exists an 8-vertex outerplanar graph that has no regular OOR.*

**Proof.** Consider the 6-vertex outerplanar graph  $G$  in Figure 21. Up to rotation and mirroring, it has only two regular OORs, which we tested using a variant of the SAT formulation described in Section 3. We call the resulting OORs Type 1 if the brown edge passes through the center of the regular hexagon, and Type 2 if the purple edge does, see Figure 21. Let  $H$  be a supergraph of  $G$  such that the two new vertices  $u$  and  $w$  are incident to the endpoints of the brown and the purple edge, respectively; see Figure 2b. None of the possibilities for adding  $u$  and  $w$  into the cyclic order of the vertices of  $G$  in Figure 21 yields a regular OOR since in each case one of the non-edges incident to  $u$  or to  $w$  (red dashed in Figure 22) lies

completely in the interior of the drawing. The vertex orders in Figure 22 satisfy the gap condition, but do not admit regular OORs. ◀



■ **Figure 21** An outerplanar graph  $G$  and its regular OORs.



■ **Figure 22** All possibilities for adding  $u$  and  $w$  into the cyclic order of the vertices of  $G$  in Figure 21. In each drawing, the red dashed non-edge misses the outer face.

## 6 Open Problems

We leave the following problems open.

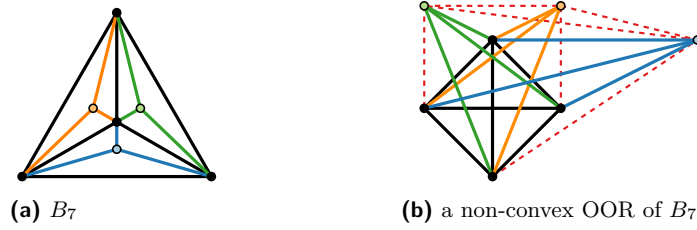
- What is the complexity of deciding whether a given graph admits an OOR?
- Is the gap condition sufficient, i.e., does every graph with a cyclic vertex order satisfying the gap condition admit a convex OOR?
- Does every graph that admits a *convex* OOR also admit a *circular* OOR?
- Does every outerplanar graph admit a (reducible) convex OOR?
- Does every connected cubic graph *except the Peterson graph* (see Figure 6) admit a convex OOR?
- We have shown that every 2-tree and hence, every graph of treewidth 2, admits a reducible OOR. Berman et al. [4] showed that there is a planar graph of treewidth 4 (see Figure 3) that does not admit an OOR. What about (planar) graphs of treewidth 3? The smallest 3-tree that does not admit a *convex* OOR is the (planar) graph with seven vertices shown in Figure 23. We verified this using the SAT formula described in Section 3.

In particular, we conjecture the following:

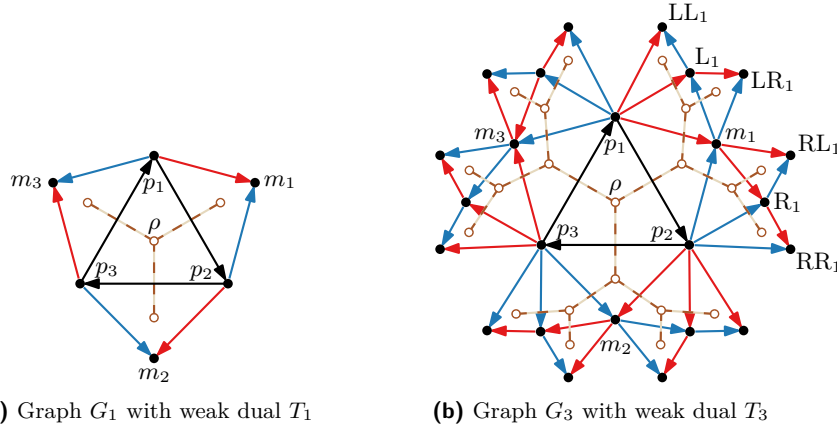
- ▶ **Conjecture 13.** *Every outerplanar graph admits a reducible circular OOR.*

The general idea is to show this only for one (infinite) family of outerplanar graphs and to obtain the result for all outerplanar graphs via reducibility. In the family  $(G_h)_{h \geq 1}$  that we propose, the graph  $G_h$  is the *complete outerplanar 2-tree* of height  $h$ . In the weak dual tree of this graph, all dual vertices have degree either 3 or 1, and one dual vertex (the root) has distance  $h$  to every leaf, see Figure 24.

For a parameter  $0 < f \leq 1/2$ , we then construct a circular outside-obstacle representation of  $G_h$  as follows. Let  $p_1, p_2$ , and  $p_3$  be the vertices of the triangle corresponding to the root of



■ **Figure 23** The smallest 3-tree  $B_7$  that does not admit a convex OOR.



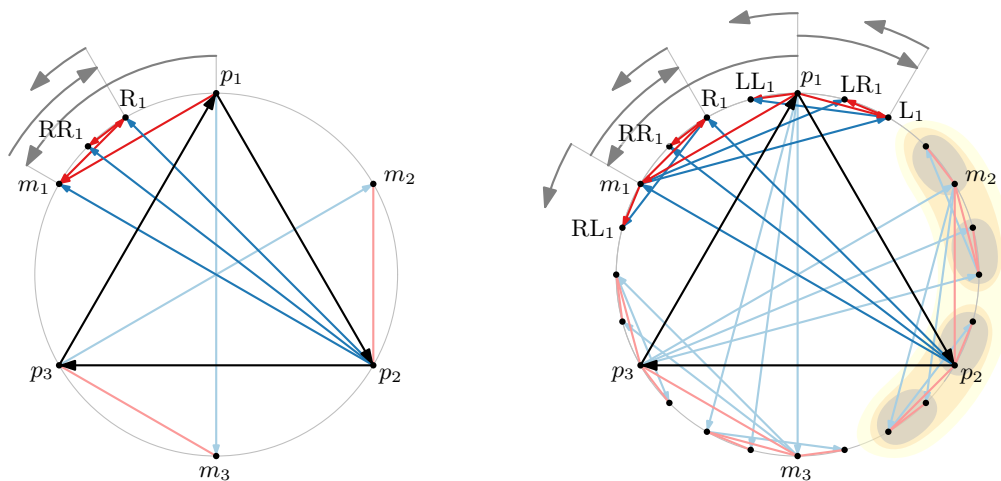
■ **Figure 24** Graph  $G_h$  with weak dual  $T_h$  (brown dashed edges) for  $h \in \{1, 3\}$ . In each vertex, the incoming edge from the primary (secondary) parent is drawn as a solid blue (red) arrow. Given the labels in  $G_1$ , the new vertices in  $G_2$  are labeled  $L_i$  ( $R_i$ ) if they are stacked to the left (right) of  $m_i$ . For  $h \geq 3$ , the new vertices are labeled by appending L or R, respectively, to the label of the parent with the longer label. (The subscript moves to the end of the label.) Hence, the label of a vertex  $v$  describes the path in  $T_h$  from the root  $\rho$  to the face that was created by adding  $v$ .

the weak dual tree. Place  $p_1$ ,  $p_2$ , and  $p_3$  with equal distances on the circle. For  $j > 0$ , place each level- $j$  vertex  $v$  clockwise  $(-f)^j \cdot 120^\circ$  away from its primary parent; see Figure 25. So for odd  $j$ ,  $v$  is placed right before its primary parent, and for even  $j$ , right after its primary parent (in clockwise order).

The intuition behind this construction is that every non-edge either already goes through a gap region for  $f = 1/2$ , or moves towards one when we decrease the value of  $f$  (which clusters the drawing). One would then have to show that, for every  $h \geq 1$ , there exists a value  $f_{\max}(h)$  such that the drawing defined above is an OOR (by Lemma 4). Finding a recursive proof, however, turned out to be challenging. On the other hand, it is comparably easy to show that the construction is reducible.

## References

- 1 Hannah Alpert, Christina Koch, and Joshua D. Laison. Obstacle numbers of graphs. *Discrete Comput. Geom.*, 44(1):223–244, 2010. doi:10.1007/s00454-009-9233-8.
- 2 Martin Balko, Steven Chaplick, Siddharth Gupta, Michael Hoffmann, Pavel Valtr, and Alexander Wolff. Bounding and computing obstacle numbers of graphs. *SIAM J. Discrete Math.*, 38(2):1537–1565, 2024. URL: <https://arxiv.org/abs/2206.15414>, doi:10.1137/23M1585088.



■ **Figure 25** Constructing a circular outside-obstacle representation of  $G_3$  for  $f = 1/2$ .

- 3 Martin Balko, Josef Cibulka, and Pavel Valtr. Drawing graphs using a small number of obstacles. *Discrete Comput. Geom.*, 59(1):143–164, 2018. doi:10.1007/s00454-017-9919-2.
- 4 Leah Wrenn Berman, Glenn G. Chappell, Jill R. Faudree, John Gimbel, Chris Hartman, and Gordon I. Williams. Graphs with obstacle number greater than one. *J. Graph Algorithms Appl.*, 21(6):1107–1119, 2017. doi:10.7155/jgaa.00452.
- 5 Steven Chaplick, Fabian Lipp, Ji-won Park, and Alexander Wolff. Obstructing visibilities with one obstacle. In Yifan Hu and Martin Nöllenburg, editors, *Proc. 24th Int. Symp. Graph Drawing & Network Vis. (GD'16)*, volume 9801 of *Lect. Notes Comput. Sci.*, pages 295–308. Springer-Verlag, 2016. URL: <http://arxiv.org/abs/1607.00278>, doi:10.1007/978-3-319-50106-2\_23.
- 6 Vida Dujmović and Pat Morin. On obstacle numbers. *Electr. J. Combin.*, 22(3):paper #P3.1, 7 pages, 2015. URL: <http://arxiv.org/abs/1308.4321>, doi:10.37236/4373.
- 7 Oksana Firman, Philipp Kindermann, Jonathan Klawitter, Boris Klemz, Felix Klesen, and Alexander Wolff. Outside-obstacle representations with all vertices on the outer face. In Patrizio Angelini and Reinhard von Hanxleden, editors, *Proc. 30th Int. Symp. Graph Drawing & Network Vis. (GD'22)*, volume 13764 of *Lect. Notes Comput. Sci.*, pages 432–440. Springer-Verlag, 2023. URL: <https://arxiv.org/abs/2202.13015>, doi:10.1007/978-3-031-22203-0\_31.
- 8 Christian Goldschmied. 1-Hindernis-Sichtbarkeitsgraphen von kubischen Graphen. Bachelor's thesis, Institut für Informatik, Univ. Würzburg, 2021. URL: <http://www1.pub.informatik.uni-wuerzburg.de/theses/2021-goldschmied-bachelor.pdf>.
- 9 León Lang. Regelmäßige Außenhindernisrepräsentation von kleinen planaren Graphen. Bachelor's thesis, Institut für Informatik, Univ. Würzburg, 2022. URL: <http://www1.pub.informatik.uni-wuerzburg.de/theses/2022-lang-bachelor.pdf>.
- 10 Padmini Mukkamala, János Pach, and Dömötör Pálvölgyi. Lower bounds on the obstacle number of graphs. *Electr. J. Combin.*, 19(2):paper #P32, 8 pages, 2012. doi:10.37236/2380.
- 11 Padmini Mukkamala, János Pach, and Deniz Sariöz. Graphs with large obstacle numbers. In Dimitrios M. Thilikos, editor, *Proc. Conf. Graph-Theoretic Concepts Comput. Sci. (WG'10)*, volume 6410 of *Lect. Notes Comput. Sci.*, pages 292–303. Springer-Verlag, 2010. doi:10.1007/978-3-642-16926-7\_27.
- 12 János Pach and Deniz Sariöz. On the structure of graphs with low obstacle number. *Graphs & Combin.*, 27(3):465–473, 2011. doi:10.1007/s00373-011-1027-0.